Cold Regions Science and Technology, 16 (1989) 45–62
Elsevier Science Publishers B.V., Amsterdam — Printed in The Netherlands

A DIFFERENTIAL FLOW MODEL FOR POLYCRYSTALLINE ICE

S. Shyam Sunder and Mao S. Wu
Massachusetts Institute of Technology, Department of Civil Engineering, Room 1-274, Cambridge, MA 02139 (U.S.A)

(Received January 7, 1988; revised and accepted June 17, 1988)

ABSTRACT

A differential model is proposed for the pure flow of polycrystalline ice. The theory is based on the concept of state variables and accounts for two deformation-rate mechanisms: (i) transient flow, associated with generally reversible isotropic and kinematic hardening, and (ii) steady-state flow, associated with irreversible viscous deformation. Dimensional requirements for creep as well as constant deformation-rate stress–strain response are satisfied. Correspondence is established between constant-stress creep and constant strain-rate tests. The uniaxial model contains a total of six parameters and follows experimental data on the creep of fresh-water polycrystalline ice obtained by Jacka (1984), Sinha (1978), and Brill and Camp (reproduced in Sinha, 1979).

1. INTRODUCTION

Boundary value problems in applied ice mechanics involving multiaxial states of stress and complex loading histories, such as those encountered during ice–structure interaction, are increasingly being solved using numerical models including the finite element method (Jordaan, 1986). Constitutive models are required to characterize the ice deformation by viscoelastic flow in numerical simulations.

In problems where only "steady-state" flow is of interest, an elastic power-law creep model of ice (sometimes without the elastic component) is adequate. Glen's (1955) power-law is commonly used in engineering applications where compressive stresses lie in the range of 0.2 to 2 MPa. Palmer (1967) has presented the multiaxial generalization of the power-law for incompressible flow of isotropic ice. By defining a scalar-valued potential function for power-law creep that is analogous to the Hill-criterion of plastic yield, Shyam Sunder et al. (1987) have presented an orthotropic model of incompressible flow.

Both the elastic and "transient" flow behavior of ice, however, are of great importance in a broad range of ice mechanics problems (Gold, 1977, Sinha et al., 1987). Several investigators have studied this problem in recent years. For example, Sinha (1978, 1979) has proposed a creep-compliance function for fresh-water polycrystalline (S-2) ice that is nonlinearly dependent on time. For loading conditions other than constant-stress creep, Sinha (1983) adopts a particular generalization of Boltzmann's superposition principle. On the other hand, Le Gac and Duval (1980) have proposed multiaxial constitutive relations based on state variable theory for modeling the isotropic and kinematic hardening phenomena governing nonelastic deformation in polycrystalline ice. Considering deformation mechanisms in ice, Ashby and Duval (1985) have subsequently developed a spring–dashpot model based on a two-bar truss analogy which they show to be equivalent to a kinematic hardening model.

Constitutive models for describing isotropic and kinematic hardening in materials undergoing deformation originated from the work of Hill (1950), Prager (1955) and Hodge (1957) on incremental visco-plasticity. More recent developments based on state variable theory are associated with Chaboche and Rousselier (1983), Miller (1976), and Hart (1976). Le Gac and Duval (1980) explicitly refer

0165-232X/89/$03.50

to the work of Hart (1976) and Miller (1976) in the development of their model.

This paper presents a differential model for the deformation of polycrystalline ice. Flow (or creep) is modeled in terms of two nonlinear deformation-rate mechanisms: the first mechanism governs the transient deformation-rate (also called "primary" creep under constant-stress loading) which decays to zero as both an internal elastic back-stress and a drag-stress measure increase asymptotically; the second mechanism, which is modeled in terms of the well-known power-law, governs the steady-state viscous deformation-rate. The evolution of the back- or rest-stress contributes to kinematic hardening, while that of the drag-stress contributes to isotropic hardening.

This model departs from prior formulations based on state variable theory since isotropic and kinematic hardening are directly associated with the transient component of deformation. For small strains and rotations, this allows an additive decomposition of the creep strain into a steady-state (viscous) component and a transient component. Consequently, a direct link can be established between the type(s) of hardening and the reversibility of the strains. For example, when both types of hardening or just kinematic hardening are present, the steady-state component is "irrecoverable". However, the transient strain is "recoverable" on unloading since equilibrium requires the internal *elastic* back-stress to reduce to zero. These time-dependent elastic strains represent delayed elasticity or anelasticity. On the other hand, if only isotropic hardening is present, both strain components are "irrecoverable".

The proposed formulation can be expressed in terms of certain dimensionless variables, identified by Ashby and Duval (1985), that are required to construct master-curves, respectively for the creep and constant strain-rate response of polycrystalline ice. The differential model follows creep data on ice, specifically the comprehensive uniaxial experimental data of Jacka (1984) for dense isotropic polycrystals, and of Sinha (1978) for transversely-isotropic columnar-grained (S-2) ice. Predictions of the ratio of transient (delayed elastic) strain to total strain agree qualitatively with Sinha's (1979) model if grain-size effects are taken into account. Correspondence between constant-stress creep and constant strain-rate tests, as observed in uniaxial compression tests at $-5°C$ on fine-grained isotropic ice by Mellor and Cole (1982, 1983), is demonstrated for deformation involving pure flow.

In general, numerical integration is necessary to solve the governing differential equations for the constitutive model since both isotropic and kinematic hardening are history-dependent phenomena. However, in the present formulation, it is possible to derive closed-form analytical solutions for the creep-compliance function and the recovery response when only kinematic hardening is present.

2. FORMULATION OF DIFFERENTIAL MODEL

Physical basis of deformation model

There is general agreement, based on theoretical and experimental work, that at least two thermally activated deformation systems, a soft system and a hard system, are present during the flow of freshwater polycrystalline ice (Sinha, 1979; Ashby and Duval, 1985). They may be: (a) grain boundary sliding (with diffusional accommodation) and basal slip, or (b) basal slip and slip on a non-basal plane. A combination of these processes could be present as well.

Initially, the solid resists the applied stresses in an elastic manner and then flow begins on the soft and hard systems. However, flow, particularly on the easy soft system, causes the build-up of internal elastic stresses. This may occur as a result of grain boundary sliding next to grains poorly aligned for deformation or dislocation pile-ups at the boundaries of such grains. Dislocation pile-ups at grain boundaries have been observed in ice through scanning electron microscopy (Sinha, 1987). The internal elastic stresses, termed *back-* or *rest-stresses*, resist flow. In addition, internal *drag-stresses* which resist dislocation fluxes are generated in annealed materials undergoing flow. The increase in drag-stresses is the outcome of: (i) creep resistant substructures, i.e., sub-grains and cells, formed by grain boundary sliding or dislocation movement, and (ii) dislocation entanglement, dipole formation and kink band formation during slip (particularly on the basal plane).

A detailed understanding of evolving structural and stress states on the deformation of polycrystalline materials is unavailable at the present time. For example, only recently has an attempt been made to model the primary creep process resulting from sub-cell formation using sub-cell size and misorientation as state variables (Derby and Ashby, 1987). However, it is well-known than an increasing drag-stress contributes to isotropic hardening, while an increasing rest-stress contributes to kinematic hardening. Both types of hardening are macro-scale manifestations of physical mechanisms occurring on the micro-scale, and are exhibited by metals (Hart, 1976), concretes (Chen, 1982), and ice (Le Gac and Duval, 1980).

Classical theories of incremental visco-plasticity generally employ the concepts of an initial yield surface and subsequent loading surfaces in constitutive formulations. The loading function depends on the state of stress and strain as well as the history of loading, and is described by a hardening rule, generally of three types: isotropic, kinematic and mixed hardening. In isotropic hardening (Hill, 1950), the loading surface expands uniformly without distortion during flow, as shown schematically in Fig. 1a. The magnitude of expansion is indepedent of the direction of straining. The drag-stress, therefore, may be expressed as a scalar variable. In kinematic hardening (Prager, 1955), the loading surface translates as a rigid-body in stress space while maintaining its original size, shape and orientation (see Fig. 1b). This type of hardening induces directionally dependent material properties, referred to as deformation-induced anisotropy. The Bauschinger effect in metals is an example of kinematic hardening. Because of the directionality of translation in a nine-dimensional stress space, the back-stress is a second-rank tensor quantity. A combination of kinematic and isotropic hardening (Hodge, 1957) leads to the more general mixed-hardening rule in which the loading surface experiences both translation and uniform expansion.

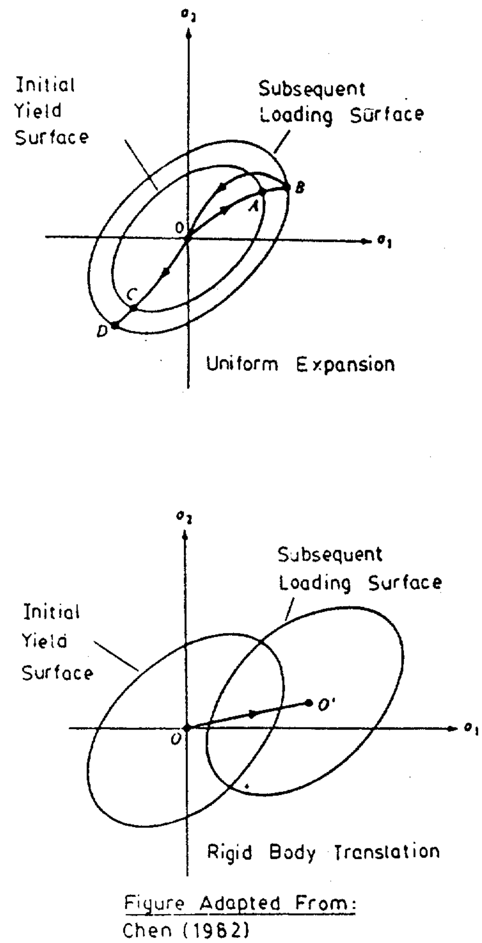

Fig. 1. (a) Isotropic and (b) kinematic hardening in classical theory of visco-plasticity.

Mathematical formulation

The model development considers the present state of the material to be dependent only on current values of the state variables, which include *observable* variables (such as total strain and temperature) and a set of *internal* variables. It follows that the effects of past history are accounted for by the state variables. The constitutive relations seek to relate the strain-rate to the state variables. Considering only small strains and small rotations, the total strain-rate is additively decomposed, i.e.:

$$\dot{\epsilon} = \dot{\epsilon}_e + \dot{\epsilon}_t + \dot{\epsilon}_v \qquad (1)$$

where the three terms on the right-hand-side represent instantaneous elasticity, transient flow, and steady-state or viscous flow, respectively. The elastic strain-rate is related to the stress-rate by a hypoelastic constitutive law of grade zero, i.e., the material-response moduli are constants (Truesdell, 1955). The nonelastic or creep strain-rate, i.e., the sum of transient and viscous strain-rates, in general may be expressed as:

$$\dot{\epsilon}_{cr}=\hat{\dot{\epsilon}}_{cr}(\sigma, T,\alpha_n) \tag{2}$$

where σ and T are state variables representing the Cauchy stress and the absolute temperature, respectively, and α_n is a list of n internal variables characterizing the flow resistance offered by the internal microstructural state of the material. In the proposed model, the internal variables are the scalar drag-stress and the back-stress tensor. The three component strain-rates are further described in what follows.

The instantaneous elastic strain, ϵ_e, is related to the stress, σ, through the Young's modulus, E, and the stress-temperature modulus, β, of polycrystalline ice. This relationship may be expressed in rate form as:

$$\dot{\epsilon}_e=\dot{\sigma}/E+\beta\dot{T}/E \tag{3}$$

where $E=\hat{E}(T)$ and $\beta=\hat{\beta}(T)$. Under isothermal conditions the last term in eqn. (3) is zero.

The viscous strain, ϵ_v, which is associated with "secondary" creep or steady flow conditions, follows the well-known Norton-type power-law of Glen (1955), i.e.,

$$(\dot{\epsilon}_v/\dot{\epsilon}_o)=(\sigma/V)^N \tag{4}$$

where N is the power-law index, $\dot{\epsilon}_o$ is a reference strain-rate (may be set equal to unity without loss of generality), and V is a temperature-dependent factor representing the stress corresponding to the reference strain-rate. Equation (4) assumes that the viscous strain-rate depends only on stress and temperature. The power-law formulation is generally considered to be adequate for the stress and temperature ranges (i.e., 0.2 to 2 MPa and -10°C to -50°C, respectively) encountered in most ice engineering problems. At higher stresses and rates of loading where microcracking may be dominant during deformation, the power-law can be used in conjunction with damage mechanics (Wu and Shyam Sunder, in prep.) to describe ice behavior. The validity of the power-law with a constant value of N greater than one has been questioned at very low stresses and strain-rates (Mellor, 1980, Hallam and Sanderson, 1987).

The temperature dependence of the stress-factor V is characterized by an Arrhenius activation energy law, i.e.:

$$V=V_o \exp(Q/NRT) \tag{5}$$

where T is the temperature in Kelvin, V_o is a temperature-independent constant, Q is the activation energy, and R is the universal gas constant equal to 8.31 J mol^{-1}K^{-1}. The Arrhenius equation is generally considered to be invalid at temperatures close to the freezing point (e.g. above -10°C) in polycrystalline ice due to the increase in Q with temperature (Barnes et al., 1971, Gold, 1983). Mellor (1980) has suggested the use of eqn. (5) with an apparent value of Q taken from experimental data, or some empirical law of the form $V=V_o \exp(k\theta/N)$, where k is a constant and θ is the number of degrees departure from a 0°C datum.

Noting eqn. (2), the transient strain-rate $\dot{\epsilon}_t$ is taken to follow a Norton-type power-law driven by a reduced-stress measure, σ_r, i.e.,

$$(\dot{\epsilon}_t/\dot{\epsilon}_o)=(\sigma_r/V)^N=\left(\frac{\sigma-R}{BV}\right)^N \tag{6}$$

where the internal variables R and B represent the back-stress and the non-dimensional drag stress, respectively. Implicit in the formulation of eqn. (6) are the assumptions that: (i) the exponent N is the same as that for steady flow in eqn. (4), and (ii) the temperature dependence of the transient deformation-rate, represented by the parameter V, is given by an Arrhenius law with an activation energy equal to that for steady flow.

The former assumption considers the underlying flow law to be the same for both deformation-rate mechanisms, the only difference being the existence of the drag- and back-stresses in the case of transient flow. However, different values of N may be appropriate for the transient and viscous flow laws if they are strongly supported by experimental data, which currently are not available. For columnar-grained polycrystalline (fresh-water) ice this assumption can also be inferred from the numerical values for parameters in Sinha's (1978) time-hardening model, and for dense isotropic polycrystals from the kinematic hardening model of Ashby and

Duval (1985). In relation to the second assumption, Sinha (1978) has shown that the activation energy for transient flow (equal to 67 kJ mol^{-1}) agrees with Gold's (1973) data for steady flow (65 kJ mol^{-1}) in the same type of ice for temperatures ranging between $-5°C$ and $-40°C$.

Evolution equations must be specified for R and B, which are the history-dependent internal variables representing transient flow. The rate of change of these variables, like the creep strain-rate in eqn. (2), is also a function of the stable variables (σ, T,α_n). In classical formulations, the evolution equations follow Bailey–Orowan type of expressions (Orowan, 1946; Chaboche and Rousselier, 1983), i.e.:

$$\dot{R}=h_1\,\dot{\epsilon}_{cr}-f_1(R,T)=\hat{\dot{R}}(\sigma,R,B,T) \qquad (7)$$

$$\dot{B}=h_2\,\dot{\epsilon}_{cr}-f_2(B,T)=\hat{\dot{B}}(\sigma,R,B,T) \qquad (8)$$

where (h_1, h_2) are strain-hardening functions, and (f_1,f_2) are static recovery-rate functions. At steady state, the evolution-rates decay to zero. Typically (h_1,h_2) are taken as constants for static thermal recovery, but they may be functions of the state variables if dynamic recovery (Kocks, 1976) is modeled. Various forms of eqns. (7) and (8) have been used by Miller (1976), Hart (1976) and Anand (1982, 1985) for metals, and by Le Gac and Duval (1980) for polycrystalline ice. The appropriateness of such expressions can only be measured by the success with which the predicted creep or stress–strain responses compare with available experimental data, since by definition *internal* variables cannot be observed or directly measured.

In the proposed model, the creep strain is decomposed into a transient (generally recoverable) and a viscous (irrecoverable) component. The stress appears in the evolution equations only through the reduced stress or the stress-difference, i.e. ($\sigma-R$), as in eqn. (6). In a manner similar to the formulation of eqns. (7) and (8), the rates of change of R and B are postulated to be linearly proportional to the transient strain-rate, i.e.:

$$\dot{R}=AE\,\dot{\epsilon}_t \qquad (9)$$

$$\dot{B}=HE\,\dot{\epsilon}_t \qquad (10)$$

Note that recovery is implicit in the expression for transient strain-rate. Steady state is reached when the transient strain-rate vanishes and the evolution rates decay to zero. The initial value of R is zero for an annealed material or for a material that has recovered from prior loading. On the other hand, the initial value of B, i.e. B_o, may represent the annealed state of the material or some level of initial hardening introduced by pre-straining. The parameter A is a temperature-independent and dimensionless constant, while H is a temperature-independent factor with units of reciprocal stress.

Under creep loading, R increases asymptotically to a value equal to the applied stress, at which point transient flow ceases. In the case of constant strain-rate loading, R approaches the steady-state stress asymptotically. The maximum value of transient strain in both these cases is given by $\epsilon_{t,max}=\sigma/AE$. For the same loading conditions, the drag-stress reaches some maximum value, implying that the isotropic resistance to transient flow is not unbounded.

Under reversed or cyclic loading, R alternates between positive and negative values, i.e., the physical processes associated with kinematic hardening relax locally, thus limiting the magnitude of hardening in the material. The drag-stress increases during uniaxial loading (where loading is defined as an increase in the magnitude of the transient strain). If unloading occurs, i.e., the magnitude of the transient strain decreases, the sign of eqn. (10) is reversed and the drag-stress decreases. The decrease in drag-stress during unloading indicates a decreasing resistance to grain boundary sliding and dislocation fluxes. This may arise from a spatial bias in the distribution of defects generated by isotropic hardening which favors regions of high back-stress concentration.

In the orthotropic generalization of the proposed model, the instantaneous elastic deformation may be described by the classical theory of elasticity (see, for example, Lekhnitskii, 1963). Rabotnov (1969) and Betten (1981) have shown that three-dimensional constitutive relations for creep can be derived by expressing the creep-rate as an isotropic function of the stresses, *or* from the assumption of the existence of a creep potential.

If the latter approach is adopted, the viscous deformation-rate may be derived by applying the normality principle to a scalar-valued flow potential expressed in terms of an equivalent-stress measure for incompressible orthotropic materials. The equivalent-stress is similar in form to that of Hill (1950) for plastic yield in metals and Hart (1976) for the nonelastic deformation of metals at elevated temperatures. The transient deformation-rate may be derived similarly, i.e., by applying normality to a flow potential expressed in terms of the equivalent reduced-stress measure and assuming incompressibility of transient flow which, though not strictly true, is a reasonable assumption according to Sinha (1987).

This approach eliminates the need for an integral formulation under variable loading histories or multiaxial loading and for generalizing the superposition assumption for nonlinearly viscoelastic materials. The orthotropic formulation derived on the basis of the foregoing arguments is presented by Shyam Sunder and Wu (in prep.).

Model formulation in dimensionless variables

For the special cases of constant-stress and constant strain-rate loading, Ashby and Duval (1985) have suggested that unique relationships exist between certain dimensionless variables. Such relationships are predicted by the proposed model as shown below.

For creep of polycrystalline ice at constant applied stress, Ashby and Duval (1985) have considered the following dimensionless variables for strain, strain-rate, time, and the back-stress:

$$\tilde{\epsilon}=\epsilon E/\sigma \tag{11}$$

$$\tilde{\dot{\epsilon}}=\dot{\epsilon}/\dot{\epsilon}_v \tag{12}$$

$$\tilde{t}=t\dot{\epsilon}_v E/\sigma \tag{13}$$

$$\tilde{R}=R/\sigma \tag{14}$$

Substituting eqns. (11)–(14) in eqns. (3), (4) and (6) yields:

$$\tilde{\epsilon}_e=1 \tag{15}$$

$$\tilde{\epsilon}_v=\tilde{t} \tag{16}$$

and

$$\tilde{\dot{\epsilon}}_v=1 \tag{17}$$

$$\tilde{R}+B\tilde{\epsilon}_t^{1/N}=1 \tag{18}$$

The dimensionless evolution equations can then be expressed as:

$$\dot{\tilde{R}}=A\tilde{\dot{\epsilon}}_t \tag{19}$$

$$\frac{\mathrm{d}B}{\mathrm{d}\tilde{t}}=\tilde{H}\frac{\tilde{\dot{\epsilon}}_t}{1-\tilde{R}} \tag{20}$$

where $H=\tilde{H}/(\sigma-R)$ in eqn. (10). This formulation for H satisfies the dimensional requirements imposed by experimental data on the creep of polycrystalline ice. It is also consistent with the formulation for the evolution-rates of the internal variables, which like the transient strain-rate, depend on the stress-difference $(\sigma-R)$. In the above equations, the differentiation is with respect to dimensionless time. Equations (15)–(20) show that the model predicts a unique relationship between the dimensionless variables and is independent of applied stress level and temperature.

Under constant strain-rate loading, the model predicts that a unique relationship exists between dimensionless stress $\tilde{\sigma}$ and dimensionless time $\tilde{t}$, independent of the applied strain-rate $\dot{\epsilon}_a$ and temperature. Consider the following dimensionless variables for stresses, time, and strains, as suggested by Ashby and Duval (1985):

$$\tilde{\sigma}=\frac{\sigma}{\sigma_{\min}};\ \tilde{R}=\frac{R}{\sigma_{\min}} \tag{21}$$

$$\tilde{\epsilon}_e=\frac{\epsilon_e E}{\sigma}=1;\ \tilde{\epsilon}_v=\frac{\epsilon_v E}{\sigma};\ \tilde{\epsilon}_t=\frac{\epsilon_t E}{\sigma};\ \tilde{\epsilon}=\frac{\epsilon E}{\sigma} \tag{22}$$

$$\tilde{t}=\frac{t\dot{\epsilon}_a E}{\sigma_{\min}}=\tilde{\epsilon}\tilde{\sigma} \tag{23}$$

where $\epsilon=t\dot{\epsilon}_a$ and $\sigma_{\min}$ is the stress corresponding to the applied strain-rate given by Glen's power-law, i.e.,

$$\sigma_{\min}=V(\dot{\epsilon}_a/\dot{\epsilon}_o)^{1/N} \tag{24}$$

Substituting eqns. (21)–(23) in eqns. (3), (4), (6), (9) and (10) yields:

$$\frac{d}{d\tilde{t}}[\tilde{\sigma}\,\tilde{\epsilon}_e]=\dot{\tilde{\sigma}} \tag{25}$$

$$\frac{d}{d\tilde{t}}[\tilde{\sigma}\,\tilde{\epsilon}_v]=\tilde{\sigma}^N \tag{26}$$

$$\frac{d}{d\tilde{t}}[\tilde{\sigma}\,\tilde{\epsilon}_t]=\left[\frac{\sigma-\tilde{R}}{B}\right]^N \tag{27}$$

$$\dot{\tilde{R}}=A\frac{d}{d\tilde{t}}[\tilde{\sigma}\,\tilde{\epsilon}_t] \tag{28}$$

$$\frac{dB}{d\tilde{t}}=\frac{\tilde{H}}{\tilde{\sigma}-\tilde{R}}\frac{d}{d\tilde{t}}[\tilde{\sigma}\tilde{\epsilon}_t] \tag{29}$$

where $\dot{\tilde{\sigma}}$ indicates $d\tilde{\sigma}/d\tilde{t}$, and similarly for $\dot{\tilde{R}}$. Explicit expressions for the dimensionless elastic, transient, and viscous strain-rates can be obtained by carrying out the differentiation in eqns. (25)–(27). Upon substituting eqns. (25)–(27) in eqn. (1) expressed in dimensionless form, the following equation is obtained:

$$\dot{\tilde{\sigma}}=1-\left[\tilde{\sigma}^N+\left(\frac{\tilde{\sigma}-\tilde{R}}{B}\right)^N\right] \tag{30}$$

Equations (27)–(30) can be integrated with the initial conditions of zero dimensionless stress and transient strain. As steady-state is reached (i.e., the dimensionless stress-rate, transient strain-rate, and rates of hardening decay to zero), the dimensionless stress and transient strain tend to one and $1/A$, respectively. The stress at steady-state therefore attains the value of σ_{min} given by eqn. (24). A single master-curve can be used to relate the dimensionless stress and time since the temperature-dependent factor V and the applied strain-rate have been eliminated from the equations. Comprehensive experimental data is currently lacking to verify the dimensionless relationships for deformation involving pure flow (no damage due to microcracking or microstructural changes associated with recrystallization) under constant strain-rate loading.

3. SOLUTION OF GOVERNING MODEL EQUATIONS

The nonlinear governing differential equations for the uniaxial model are defined in eqns. (1), (3), (4), (6), (9) and (10). For constant-stress creep loading, the solutions of eqns. (1), (3) and (4) are trivial. However, eqns. (6), (9) and (10) are coupled and numerical integration is necessary to compute the transient strains if both isotropic and kinematic hardening are present. If isotropic hardening is absent, i.e., B is a constant, analytical solutions can be obtained for the *nonlinear* ($N>1$) differential equations. For a general or variable loading history, the governing equations are all coupled and numerical integration is required.

Closed-form analytical solutions for creep and recovery response

The closed-form analytical solutions for the creep and recovery response when isotropic hardening is absent are derived below. These solutions provide valuable insights regarding the behavior of the model.

In an ideal creep test, the stress, σ, is applied instantaneously and the stress-rate history is a Dirac delta function, $\delta(t)$, with amplitude σ. This history is zero for all t except at $t=0$ where it is infinity such that:

$$\int_{-\infty}^{t^*}\sigma\,\delta(t)=\sigma \tag{31}$$

for $t^*>0$ and zero otherwise. Consequently, the initial strain-rate predicted by the model is also a Dirac delta function, i.e., it is equal to infinity. The amplitude of this function is σ/E, which corresponds to the instantaneous elastic strain. For time incrementally greater than zero, the strain-rate is finite and equals:

$$\dot{\epsilon}^+=(\sigma/BV)^N+(\sigma/V)^N \tag{32}$$

Equation (32) recognizes that the elastic back-stress is equal to zero initially. If the first term of the equation, representing transient flow, dominates the initial creep response, the constant B will be less than one.

The dimensionless creep-compliance function for the model, J, is the sum of the dimensionless elastic, transient and viscous strains, respectively, i.e.,

$$J=\tilde{\epsilon}_e+\tilde{\epsilon}_t+\tilde{\epsilon}_v \tag{33}$$

The dimensionless elastic and viscous strains are given in eqns. (15) and (16). The dimensionless transient strain can be analytically derived from eqns. (18) and (19) with a substitution of variables approach. In particular, define a variable q as follows:

$$q = 1 - A\,\tilde{\epsilon}_t \tag{34}$$

Then,

$$\dot{q} = -A\,\tilde{\dot{\epsilon}}_t \tag{35}$$

Substitution of eqns. (34) and (35) into eqn. (18) and a separation of variables yields:

$$\int \frac{\mathrm{d}q}{q^N} = \frac{-A}{B^N} \int \mathrm{d}\tilde{t} \tag{36}$$

Integrating eqn. (36), applying the initial condition of $\tilde{\epsilon}_t = 0$, i.e., $q = 1$, and substituting for q results in:

$$\tilde{\epsilon}_t = 1/A - [A^{N-1} + A^N/B^N(N-1)\tilde{t}]^{1/(1-N)} \tag{37}$$

Equation (33) together with eqns. (15), (16) and (37) provide a closed-form analytical solution for the dimensionless creep-compliance function. Also, by substituting eqn. (37) in eqn. (18), the dimensionless transient strain-rate can be expressed in terms of dimensionless time as:

$$\tilde{\dot{\epsilon}}_t = [B^{N-1} + A/B(N-1)\tilde{t}]^{N/(1-N)} \tag{38}$$

Equations (37) and (38) show that the dimensionless transient strain and strain-rate tend to $1/A$ and $1/B^N$ as dimensionless time tends to infinity and zero, respectively.

If creep recovery is allowed to occur at time $\tilde{t} = \tilde{t}_u$, the elastic component of the strain is recovered instantaneously while the viscous component is irrecoverable and remains unchanged with time. However, the transient strain will decay with time according to the following closed-form analytical solution that can be derived from eqns. (18) and (19) in a manner similar to eqn. (37):

$$\tilde{\epsilon}_t = [\tilde{\epsilon}_{tu}{}^{1-N} + (A/B)^N(N-1)\ (\tilde{t} - \tilde{t}_u)]^{1/(1-N)} \tag{39}$$

where $\tilde{\epsilon}_{tu}$ is the dimensionless transient strain at the time of unloading. Equation (39) shows that the dimensionless transient strain decays to zero with dimensionless time after unloading.

Numerical solutions for creep, constant strain-rate and arbitrary loading histories

In many engineering applications involving transient and viscous flow, the entire loading history has to be traced and this leads to an initial-value problem posed by the evolution equations for the internal variables and the equations for the nonelastic strain-rates. These equations are coupled, highly nonlinear, and could be mathematically stiff in certain applications (Cordts and Kollmann, 1986).

The governing equations of the uniaxial model are regarded as a coupled system of first-order ordinary differential equations. If $\dot{\epsilon}_{cr}$ and R, B represent the nonelastic strain-rate and internal variables, respectively, then in general the initial value problem can be expressed as follows:

$$\dot{R} = AE\dot{\epsilon}_t = \hat{\dot{R}}(\sigma, T, R, B) \tag{40}$$

$$\dot{B} = \tilde{H}E/(\sigma - R)\ \dot{\epsilon}_t = \hat{\dot{B}}(\sigma, T, R, B) \tag{41}$$

$$\dot{\sigma} = E(\dot{\epsilon} - \dot{\epsilon}_{cr}) = \dot{\sigma}(\sigma, T, R, B) \tag{42a}$$

or

$$\dot{\epsilon} = \dot{\sigma}/E + \dot{\epsilon}_{cr} = \hat{\dot{\epsilon}}(\sigma, T, R, B) \tag{42b}$$

where

$$\dot{\epsilon}_{cr} = (\sigma/V)^N + (\sigma_r/V)^N = \hat{\dot{\epsilon}}_{cr}(\sigma, T, R, B) \tag{43}$$

For isothermal strain-controlled tests, the unkowns are R, B and σ. The histories of these unkowns can be obtained by simultaneously integrating eqns. (40), (41) and (42a). For isothermal stress-controlled tests, the two unkowns R and B can be obtained by simultaneously integrating eqns. (40) and (41). The strain-history can then be computed from eqns. (42b) and (43).

For the uniaxial equations considered in this paper, the Runge–Kutta–Verner fifth and sixth order numerical integration algorithm is satisfactory and no numerical instability is encountered. A variable time-step may be used for generating the dimensionless creep response since the transient strain-rate, which is initially very high and requires small time-steps for accuracy of integration, decays with time and requires larger time-steps for computational efficiency. Specifically, the following time-steps are used for generating Figs. 2–11:

Figs. 2–6	:	variable time-step, but with a constant ratio of 1.38 between the current and previous time-increments;
Fig. 7	:	constant time-step of 5 s;
Fig. 8	:	constant time-step of 70 s;
Fig. 9	:	constant time-step (dimensionless) of 0.05;
Figs. 10 and 11	:	for constant strain-rate tests, a constant time-step of 10 s; for creep tests, variable time-step with a constant ratio of 1.20 between the current and previous time-increments.

4. MODEL PREDICTIONS AND EXPERIMENTAL VALIDATION

Parameter identification and estimation

The uniaxial model contains a total of six parameters: E, N, V_o, A, H and B_o. For single ice crystals and transversely-isotropic ice, five independent constants are needed to describe elastic behavior. Values for these elastic moduli are available for single crystals (Green and Mackinnon, 1956). The value of E for polycrystalline isotropic ice can be estimated from the elastic moduli of single crystals (Gammon et al., 1983). Several investigators (see, e.g., Gold, 1977) have independently shown using high-frequency sonic methods that the Young's modulus of polycrystalline fresh-water ice varies in the range of 9–11 GPa, with negligible temperature dependence between $-5°$C and $-45°$C.

Based on test data corresponding to $-10°$C and a stress-range of 0.2 to 2 MPa, Ashby and Duval (1985) have estimated the value of N to be three for the creep of isotropic polycrystals. The use of $N=3$ for isotropic polycrystalline ice at moderate stresses is supported by theoretical models which assume dislocation mobility as the rate-controlling process (Baker, 1982). Sinha (1978) has also found the same value for the stress-exponent from experimental observations.

The temperature-independent constant V_o and the activation energy Q can be estimated from creep data for various temperatures. From the values of the parameters used in Sinha's equation (1978, 1979), V_o is estimated to be 6.59 kPa for Q=67 kJ mol^{-1}.

Under constant-stress loading, the parameters A and B_o determine the maximum value of the transient strain (σ/AE) and the initial transient strain-rate $(\sigma/B_oV)^N$, respectively. The constant A can be estimated by subtracting the elastic strain and the viscous strain from the total strain when steady-state is reached. Since the total recoverable deformation is $\sigma/E+\sigma/AE$, the fully-relaxed elastic modulus, equal to the applied stress per unit maximum recoverable deformation, is given by $EA/(1+A)$. This allows A to be computed from a creep-recovery test as well. The constant B_o can be estimated from eqn. (32). This requires knowledge of the initial strain-rate and the constant V. The latter can be computed from eqn. (5), but initial strain-rates computed from experimentally-observed initial strains may be somewhat inaccurate due to measurement limitations and ambiguities in the physical interpretation of the data at small strains (see, for example, Jacka, 1984; Mellor and Cole, 1982).

The parameter $\tilde{H}$ controls the amount of isotropic hardening at a given time. Being associated with the internal variable B, it can only be estimated from the entire transient strain and strain-rate histories. Having determined V, the viscous strain and strain-rate histories are known, and the transient strains and strain-rates can then be obtained from the creep data. Integrating eqns. (9) and (10) and substituting the results in eqn. (6), yields the following expression:

$$\ln\{[(\sigma-AE\epsilon_t)/(V\dot{\epsilon}_t^{1/N})]^{N+1}-B_o^{N+1}\} =\ln\{\tilde{H}E(N+1)/V^N\} +\ln\{\int_0^t(\sigma-AE\epsilon_t)^{N-1}\mathrm{d}t\} \tag{44}$$

The quantity on the left-hand-side plotted against the second term on the right-hand-side of eqn. (44) ideally is a straight line, and $\tilde{H}$ can be computed from its intercept with the y-axis.

Comparison of the model predictions with experimental data in this paper is based on the following values for N, E, V_o and Q:

$N=3$

$E=9.50$ GPa
$V_o=6.59$ kPa
$Q=67.0$ kJ mol^{-1}

Comparison of model predictions with Jacka's creep data

Jacka (1984) has published results of uniaxial compression tests on isotropic polycrystalline ice with a mean grain size of 1.7 ± 0.2 mm. The samples were tested under constant stress ranging from 0.1 to 1.5 MPa at the following specific temperatures: -5.0, -10.6, -17.8 and -32.5°C. Figures 2, 3 and 4 show plots for Jacka's data (taken from Ashby and Duval, 1985) corresponding to $\tilde{\dot{\epsilon}}$ versus $\tilde{t}$, $\tilde{\dot{\epsilon}}$ versus $\tilde{t}$, and $\tilde{\dot{\epsilon}}$ versus $\tilde{\epsilon}$, respectively. The predictions of the model are indicated by solid lines with $A=0.0142$, $B_o=0.286$ and $\tilde{H}=0.02$. Also shown are the model predictions for no isotropic hardening using the solutions given in eqns. (15)–(17) and eqns. (37) and (38). Parameters used for generating these curves are $A=0.033$ and $B=0.402$. Note that for experimental data plotted in dimensionless form, the model predictions are independent of E, V_o and Q. The predictions of Sinha's (1978) equation as modified by Ashby and Duval (1985) are also shown in the figures.

The solid lines show that model predictions agree with the data when strain-rate is plotted against time or strain (Figs. 2 and 3). The predicted master-curve in the strain versus time plot (Fig. 4) also follows the data, but at small times the predicted strains somewhat overestimate the experimental data. With no isotropic hardening, the initial strain-rates are underestimated while the initial strains agree with the data. While the values of the parameters are unchanged for the proposed model in all three figures, the value of the parameter which equals the maximum transient strain for the modified equation (parameter A in Ashby and Duval's paper) is reduced by a factor of two in Figs. 3 and 4.

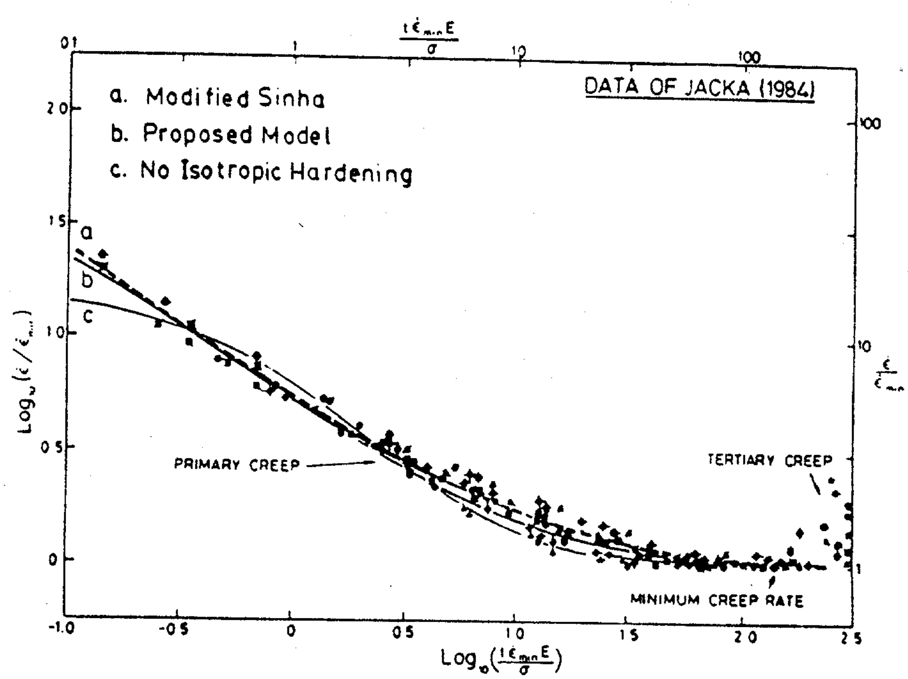

Fig. 2. Dimensionless strain-rate plotted against dimensionless time, from the data of Jacka (1984); (figure, excluding model predictions, reproduced from Ashby and Duval, 1985).

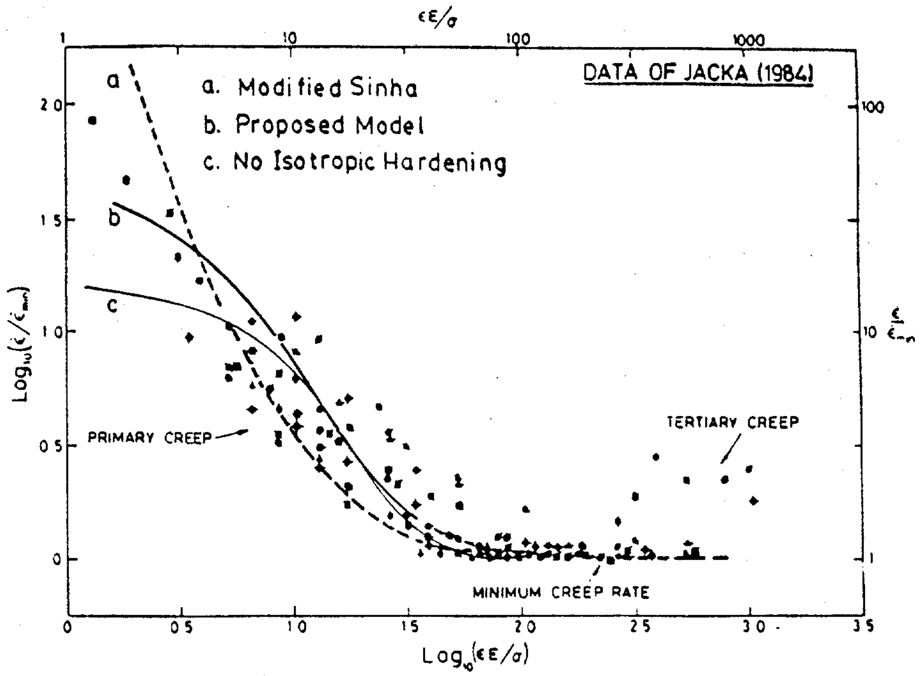

Fig. 3. Dimensionless strain-rate plotted against dimensionless strain, from the data of Jacka (1984); (figure, excluding model predictions, reproduced from Ashby and Duval, 1985).

Comparison of model predictions with Sinha's creep data

Sinha (1978) has conducted tests on the creep response of transversely-isotropic columnar-grained ice (S-2 ice) with an average grain diameter of 3 mm. The tests were conducted in the temperature range of -9.9 to -41 °C under a uniaxial compressive load of 0.49 MPa acting in the plane of transverse-isotropy. Figure 5 shows the creep strains obtained at various temperatures shifted to a reference temperature of -10°C using the shift-function derived from the Arrhenius law by Sinha (1978). The solid line indicates the model prediction with $A=0.33$, $B_o=0.0865$ and $\bar{H}=0.454$. The value of A is identical to that obtained by Sinha (1978). The experimental data and theoretical results are in agreement. Notice also that the values of A, $\bar{H}$ and B_o used for Sinha's and Jacka's data are different, reflecting differences in the ice types that were tested, i.e., isotropic and granular versus transversely-isotropic and columnar-grained, as well as the average diameters of ice grains. Such modifications to parameter values are also needed for Sinha's equation. For example, the parameter corresponding to A was determined to be 1/3 from Sinha's data, but according to Ashby and Duval (1985) values of 1/70 and 1/35 are suitable for Jacka's data.

Model prediction of ratio of transient to total strain

The parameter AE can be interpreted as an anelastic modulus (not to be confused with relaxed modulus), while BV represents the isotropic resistance to transient flow. If transient deformation is related to grain-size as postulated by Sinha (1979), then the parameters A and H will depend on grain-size. Sinha's (1979) model considers both transient strain and strain-rate to be inversely proportional to grain-size. For consistency with this formulation in making comparisons, it is necessary for the model parameters to be related to the grain-size d as follows:

$$A=d/A' \tag{45}$$

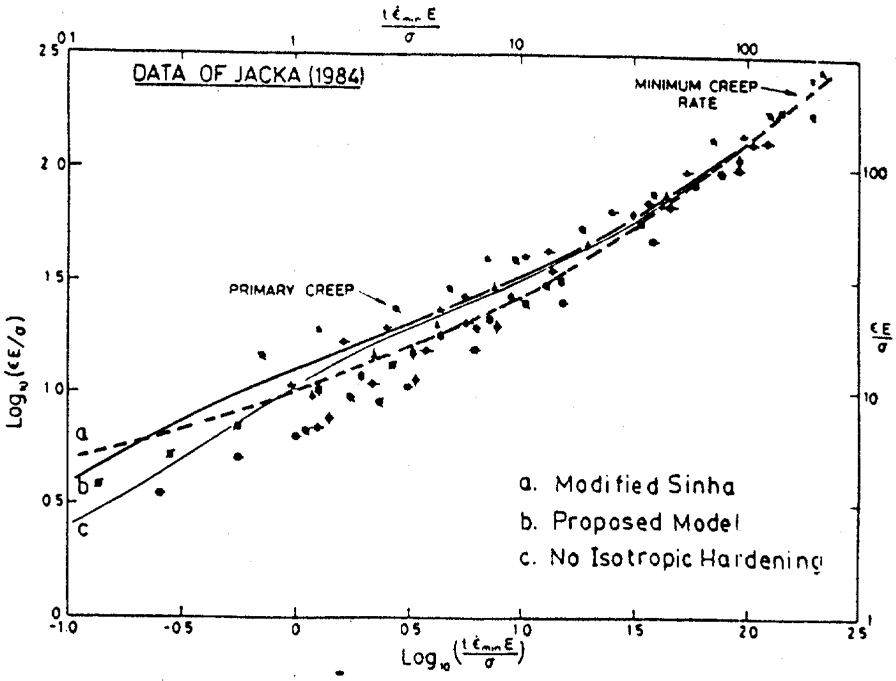

Fig. 4. Dimensionless strain plotted against dimensionless time, from the data of Jacka (1984); (figure, excluding model predictions, reproduced from Ashby and Duval, 1985).

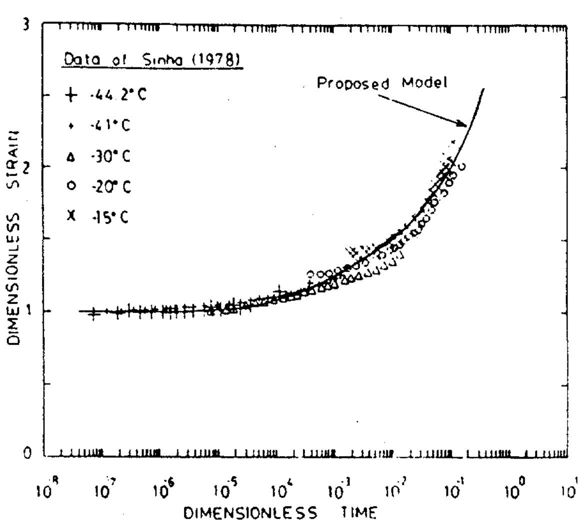

Fig. 5. Dimensionless strain plotted against dimensionless time, from the data of Sinha (1978).

$$B_o = B_o' d^{(1/N)} \tag{46}$$

$$\tilde{H} = \tilde{H}' \, d^{(N+1)/N} \tag{47}$$

where A', B_o' and $\tilde{H}'$ are grain-size independent material parameters. The values of these latter parameters are calculated from eqns. (45)–(47) respectively. For the previously determined values of A, B_o and $\tilde{H}$ (viz., 0.33, 0.0865 and 0.454) $A'=9$ mm, $B_o'=0.06$ mm$^{-1/N}$, and $\tilde{H}'=0.105$ mm$^{-(N+1)/N}$.

The analytical solutions for the case of no isotropic hardening are useful in inferring some of the characteristics of the complete model. Equations (17) and (38) show that the ratio of the (dimensionless) transient strain-rate to the viscous strain-rate decreases with increase in grain-size. The ratio also decreases with dimensionless time. According to the definitions of dimensionless time (eqn. (13)) and viscous strain-rate (eqn. (4)), the ratio must also decrease with increase in applied stress. These trends are in agreement with predictions of Sinha's equation.

The predictions of the proposed model and Sinha's equation with regard to the relative contribution of transient strain to total strain are compared below. Let the ratio of the transient strain to the total strain, γ, be defined as follows:

$$\gamma=\frac{\bar{\epsilon}_t}{\bar{\epsilon}}=\frac{\bar{\epsilon}}{\bar{\epsilon}_t+\bar{t}+1} \tag{48}$$

By solving eqns. (18)–(20), the strain dependence of γ under a constant stress load of 1 MPa at $-10°C$ for varying grain-size is predicted as shown in Fig. 6. The important features predicted by Sinha's equation such as the increasing value of γ with decreasing d, the occurrence of maximum γ at small strains, the gradual shift of the maxima towards larger strains with decreasing d, the gradual decrease in γ with increase in strain after the peak is passed, and the decreasing effect of d on γ at large strains are all observed in the figure. The actual numerical values in the figure are different from those of Sinha (1979), except at the grain-size of 3 mm which corresponds to the test data from which the model parameters are determined. Furthermore, since the relationship between the dimensionless transient strain and time is independent of temperature (eqn. (37)), it can be deduced from eqn. (48) that the evolution of γ with *dimensionless* strain for a given grain-size is unique, i.e., independent of both temperature and stress level.

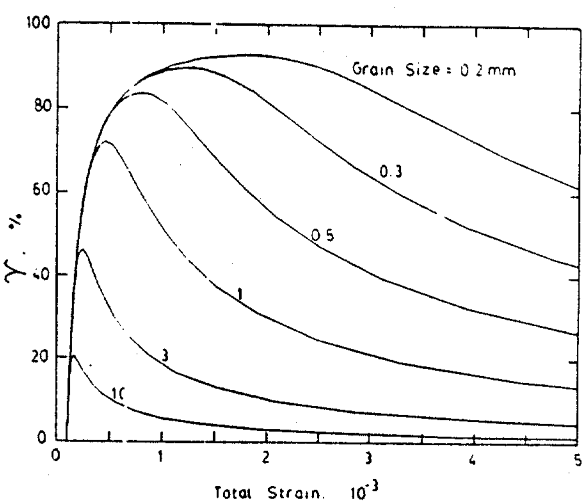

Fig. 6. Strain dependence of ratio of transient strain to total strain for various grain sizes; $\sigma=1.0$ MPa at $-10°C$.

Prediction of model response under monotonically increasing stress

The rate-sensitivity of the compressive strength of columnar-grained ice under constant cross-head displacement rates has been investigated by Sinha (1981). He conducted tests at $-10°C$ on ice with an average grain-size of 4.5 mm and under a constant cross-head displacement rate of 1.25×10^{-3} cm/s. The results were found to be representative of the constant stress-rate rather than the constant strain-rate condition.

Using the actual stress-time history shown in the upper curve of Fig. 7b (not the constant stress-rate idealization) as input, the strain–time response of the proposed model is predicted and superimposed on the test data as shown in the lower curve. The values of the hardening parameters are determined from eqns. (45)–(47) for the given grain-size and previously determined values of the grain-size independent parameters. Figure 7a shows the predicted stress versus strain response superimposed on the test data. These figures show that the predictions of the proposed model under monotonically increasing stress agree with experimental observa-

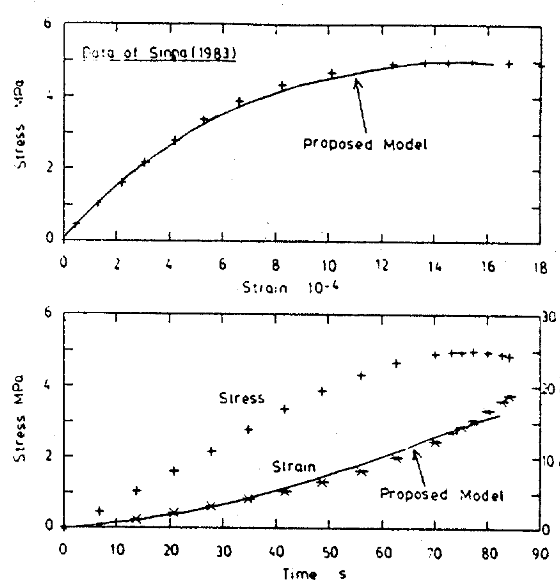

Fig. 7. (a) Stress–strain results and (b) stress and strain history for columnar-grained ice of average grain diameter of 4.5 mm at $-10°C$ and nominal strain-rate of 5×10^{-5} s^{-1} (data from Sinha, 1983).

tions. Note that parameter values, which were determined from a different data set, are kept unchanged.

Comparison of model predictions with the creep and recovery data of Brill and Camp

Figure 8 shows creep and recovery data for tests conducted on randomly oriented snow-ice by Brill and Camp (reproduced in Sinha, 1979). The three sets of data refer to tests carried out under the following conditions: curve (a) at $-5\,^{\circ}$C and 0.232 MPa, curve (b) at $-5\,^{\circ}$C and 0.125 MPa, and curve (c) at $-10\,^{\circ}$C and 0.238 MPa. The model predictions, shown in solid lines, are generated with $A'=6.5$ mm, $B_o'=0.13$ mm$^{-1/N}$ and $\bar{H}'=0.001$ mm$^{-(N+1)/N}$. The grain-sizes used for curves (a), (b) and (c) are 2.3 mm, 2 mm, and 1.5 mm respectively, which are almost identical to the values determined by Sinha (1979). Differences in the hardening parameters reflect the difference in ice types, i.e., transversely-isotropic and columnar-grained versus isotropic and granular snow-ice. The agreement between the model predictions and test data is acceptable, given that the measurement of strain recovery in ice shows large scatter (Sinha, 1982).

A major difference exists between Sinha's recovery model and the present formulation. The former can result in a decrease of the permanent/irrecoverable viscous strain and eventually lead to reversed strain (e.g., an elongation or tensile strain due to recovery from compressive creep). This is due to the particular form of the superposition principle adopted, in which the elastic and the transient strains resulting from the sudden reduction in stress are subtracted from the total strain at unloading. Recovery is thus the mirror image of the transient term in the equation for loading and as time increases it can exceed the transient creep strain at the instant of unloading. The proposed formulation does not suffer from this modeling limitation.

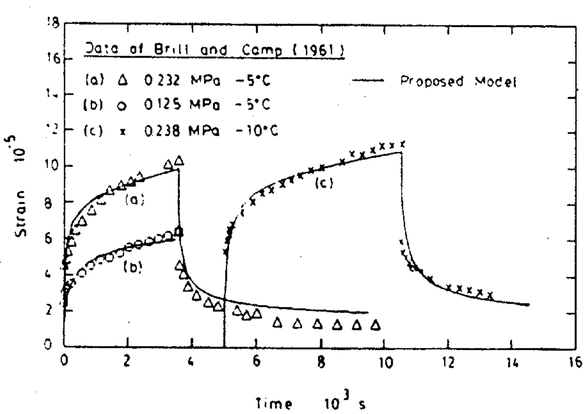

Fig. 8. Comparison between the predicted and experimental creep and recovery of snow-ice. Experimental data of Brill and Camp reproduced from Sinha (1979). The zero time of curve (c) is shifted for clarity.

Constant strain-rate tests

The dimensionless stress–time curves of the model, shown in Fig. 9a, are generated with eqns. (27)–(30). Using the relationship between dimensionless time and strain given in eqn. (23), the stress–strain curves (Fig. 9b) follow immediately. Note that the dimensionless stress–strain curves start from a dimensionless strain of unity since the limiting ratio of the total to the elastic strain at zero time (last equation of eqns. (22)) equals one. Parameter values are identical to those used for the creep data of: (a) Jacka with a grain size of 1.7 mm, (b) Sinha with a grain size of 3 mm, and (c) Brill and Camp with a grain size of 2.3 mm. The proposed model considers deformation involving only pure flow, i.e. no damage or recrystallization. Thus, correspondence as noted by Mellor and Cole (1982) can be established between constant-stress creep and constant strain-rate responses under these conditions as shown below.

First, all the curves in Fig. 9a have an initial slope of one, which corresponds to a unit-intercept on the strain axis of dimensionless strain–time creep curves (see Fig. 5). Thus, correspondence for Young's modulus is established.

A second point of correspondence is that the strength for a given strain-rate can be determined directly from a constant strain-rate test, or from a creep test in which the minimum strain-rate equals the applied strain-rate. Figure 9 shows that the dimensionless strength (maximum or steady-state flow stress in this model) is one, i.e. the strength

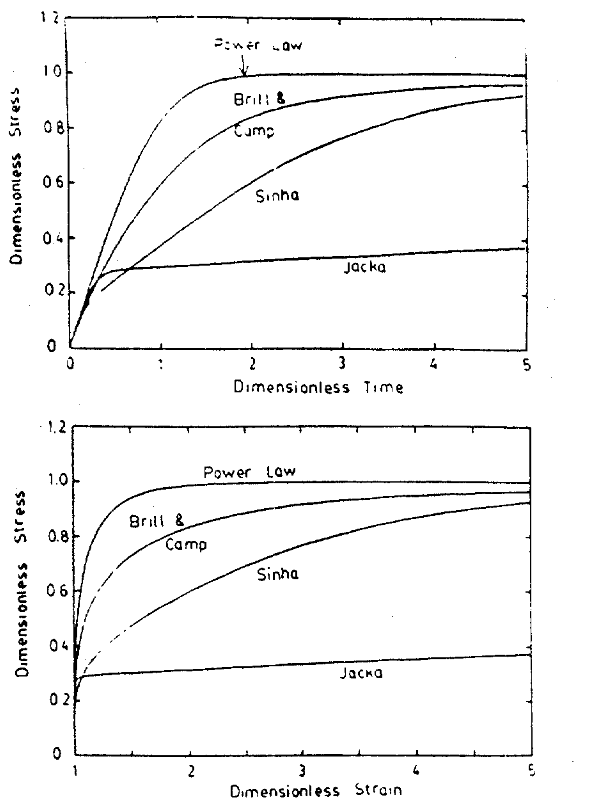

Fig. 9. (a) Dimensionless stress–time and (b) dimensionless stress–strain curves generated with parameters determined from the creep tests of Sinha (1978), Jacka (1984), and Brill and Camp (Sinha, 1979). The elastic, power-law prediction is included for comparison.

equals σ_{min} corresponding to an applied strain-rate $\dot{\epsilon}_a$. On a dimensionless strain-rate versus time creep curve (Fig. 2), the stress corresponding to $\dot{\epsilon} = \dot{\epsilon}_{min} = \dot{\epsilon}_a$, i.e., $\bar{\dot{\epsilon}} = 1$, is σ_{min} by eqns. (4) and (24). Hence the strength is, in principle, measurable from both types of test. From this it can be inferred that the variation of strength with strain-rate can also be investigated by either test.

The converse problem of estimating the minimum creep-rate for a given stress is likewise amenable to direct measurement as well as an indirect approach involving stress–strain curves. By selecting the stress–strain curve on which the strength equals the applied stress of the creep test, the required minimum strain-rate is found, again by virtue of the correspondence of eqns. (4) and (24).

In a broader view, since a consistent set of differential equations govern both creep and constant strain-rate solutions, there is complete correspondence between theoretical creep and stress–strain curves. This is confirmed by Fig. 10, which shows the construction of a stress–strain curve for the strain-rate of $10^{-6}s^{-1}$ from a family of creep curves, and by Fig. 11, which shows the construction of a creep curve for the stress of 1 MPa from a family of stress–strain curves. All curves in these two figures are generated with the model parameters derived from Sinha's (1978) data. In Fig. 10a, a horizontal straight line at the level of $10^{-6}s^{-1}$ is drawn across

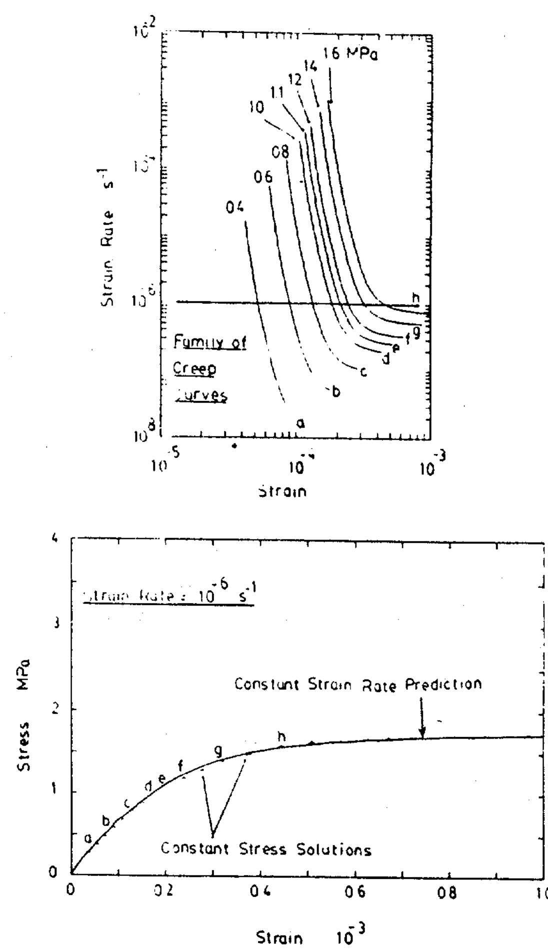

Fig. 10. (a) Transecting a family of theoretically predicted creep curves; (b) comparison of stress vs. strain relationships obtained (i) by transecting creep curves, and (ii) from theoretical constant strain-rate solution of model equations.

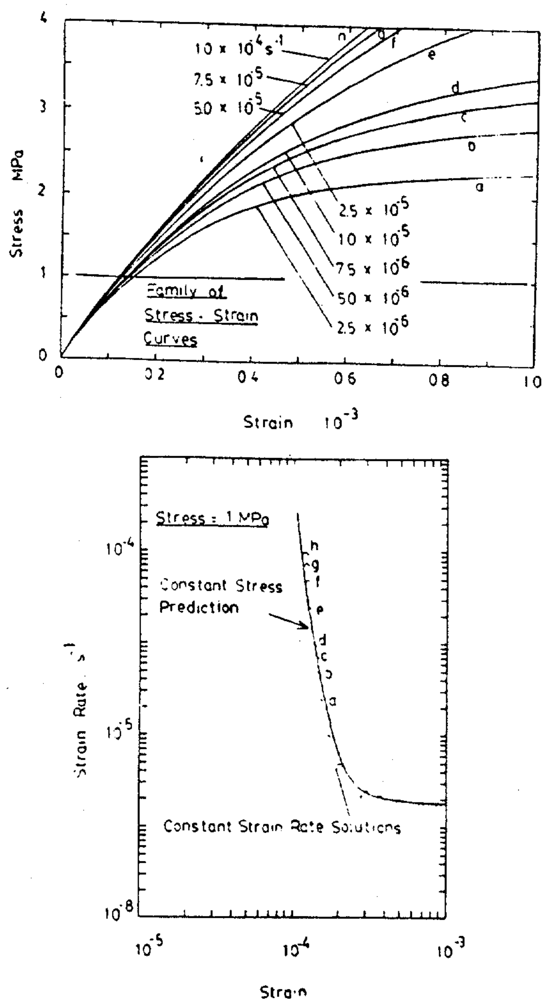

Fig. 11. (a)Transecting a family of theoretically predicted stress–strain curves; (b) comparison of strain-rate vs. strain relationships obtained (i) by transecting stress–strain curves, and (ii) from theoretical constant-stress solution of model equations.

the creep curves. Stress and strain values, read off at the points of intersection, are re-plotted as data points in Fig. 10b, which also shows the theoretical constant strain-rate prediction of the model. Allowing for errors arising from numerical integration of the model equations and from the transecting operation, it can be concluded that the proposed model satisfies the correspondence requirement. Figure 11b is obtained from Fig. 11a in an entirely analogous manner. Agreement between data points obtained by transection and the theoretical constant-stress solution again shows that the model satisfies the correspondence requirement.

5. CONCLUSIONS

A differential constitutive model for polycrystalline ice which seeks to model the underlying physical deformation mechanisms on the basis of state variable theory is presented in this paper. Instantaneous deformation is characterized by the classical theory of linear elasticity, while the steady viscous deformation-rate is described by Glen's power-law. The transient deformation-rate mechanism is modeled by the interaction between the thermally-activated soft and hard deformation systems which gives rise to an internal drag-stress and an elastic back-stress. The rate-dependent evolution of the drag- and back-stresses respectively govern isotropic and kinematic hardening in the material. Since hardening is directly related to transient deformations, the recoverability of transient strains (representative of delayed elastic or anelastic deformation) depends on the presence of a non-zero elastic back-stress. Dimensional requirements identified by Ashby and Duval (1985) for the creep and constant strain-rate response of polycrystalline ice are satisfied by the model.

The uniaxial model contains a total of six parameters that can be determined from conventional experimental testing methods for ice. The model follows creep and recovery data on ice, specifically those of Jacka (1984), Sinha (1978), and Brill and Camp (reproduced in Sinha, 1979). Predictions of the ratio of transient to total strain agree qualitatively with Sinha's equation if grain-size effects are taken into account. The response of the model under monotonically increasing stress follows the data obtained by Sinha (1983) from constant displacement-rate tests. Validation of constant strain-rate predictions suffers from a lack of comprehensive data on deformation involving pure flow (no microcracking-induced damage or recrystallization), but the proposed model predicts the correspondence between constant-stress creep and constant strain-rate response observed experimentally by Mellor and Cole (1982, 1983).

6. ACKNOWLEDGEMENTS

The authors would like to acknowledge financial support from the U.S. Army Research Office through the MIT Program for Advanced Construction Technology; BP America through the MIT Center for Scientific Excellence in Offshore Engineering; and the U.S. Department of the Interior, Minerals Management Service.

REFERENCES

Anand, L. (1982). Constitutive equations for the rate-dependent deformation of metals at elevated temperatures. ASME J. Eng. Materials Technol., 104: 12–17.

Anand, L. (1985). Constitutive equations for hot-working of metals. Int. J. Plasticity, 1; 213.

Ashby, M.F. and Duval, P. (1985). The creep of polycrystalline ice. Cold Regions Science and Technology, 11(3): 285–300.

Baker, R.W. (1982). A flow equation for anisotropic ice. Cold Regions Science and Technology, 6(2): 141–148.

Barnes, P., Tabor, D. and Walker, J.C.F. (1971). The friction and creep of polycrystalline ice. Proc. Royal Soc. London A, 324: 127–155.

Betten, J. (1981). Representation of constitutive equations in creep mechanics of isotropic and anisotropic materials. In: Ponter, A.R.S. (Ed.); Creep in Structures, Springer-Verlag, pp. 179–201.

Chaboche, J.L. and Rousselier, G. (1983). On the plastic and viscoplastic constitutive equations – Part I: Rules developed with internal variable concept. J. Pressure Vessel Technol., 105: 153–164.

Chen, W.F. (1982). Plasticity in Reinforced Concrete. McGraw-Hill, New York.

Cordts, D. and Kollman, F.G. (1986). An implicit time integration scheme for inelastic constitutive equations with internal state variables. Int. J. Numerical Methods in Engineering, 23: 533–554.

Derby, B. and Ashby, M.F. (1987). A microstructural model for primary creep. Acta Metallurgica, 35(6): 1349–1353.

Le Gac, H. and Duval, P. (1980). Constitutive relations for the non-elastic deformation of polycrystalline ice. Tryde, P. (Ed.), Proc. IUTAM Symp. Physics and Mechanics of Ice, Springer, pp. 51–59.

Gammon, P.H., Kiefte, H., Clouter, M.J. and Denner, W.W., (1983). Elastic constants of artificial and natural ice samples by Brillouin spectroscopy. J. Glaciol., 29(103): 433–460.

Glen, J.W. (1955). The creep of polycrystalline ice. Proc. Royal Soc. London, Ser. A, 228(1175): 519–538.

Gold, L.W. (1973). Activation energy for creep of columnar-grained ice. In: Whalley, E., Jones, S.J. and Gold, L.W. (Eds.), Physics and Chemistry of Ice, Roy. Soc. Canada, Ottawa, pp. 362–364.

Gold, L.W. (1977). Engineering properties of fresh water ice. J. Glaciol., 19 (81): 197–212.

Gold, L.W. (1983). Creep of columnar-grained ice at low stress. Ann. Glaciol., 4: 73–78.

Green, R.E. and Mackinnon, L. (1956). Determination of the elastic constants of ice single crystals by an ultrasonic pulse method. J. Acoustical Soc. Am., 28: 1292.

Hallam, S.D. and Sanderson, T.J.O. (1987). Advances in ice mechanics in the United Kingdom. In: Chung, J.S., Hallam, S.D., Maatanen, M., Sinha, N.K. and Sodhi, D.S. (Eds.), Advances in Ice Mechanics – 1987. ASME, Offshore Mech. Arctic Eng. Symp. Comm., Houston, Texas, pp. 1–5.

Hart, E.W. (1976). Constitutive relations for the nonelastic deformation of metals. J. Eng. Materials and Technol., 96: 193–202.

Hill, R. (1950). The Mathematical Theory of Plasticity. Oxford University Press, London.

Hodge, P.G., Jr (1957). Discussion [of Prager (1956)]. J. Appl. Mech., 23: 482–484.

Jacka, T.H. (1984). The time and strain required for the development of minimum strain rates in ice. Cold Regions Science and Technology, 8(3): 261–268.

Jordaan, I.J. (1986). Numerical and finite element techniques in calculation of ice-structure interaction. Proc. IAHR Symp. on Ice, Iowa City, Iowa, Vol. II, pp. 405–440.

Kocks, U.F. (1976). Laws of work-hardening and low temperature creep. ASME J. Eng. Materials and Technol., 98: 76–85.

Lekhnitskii, S.G. (1963). Theory of Elasticity of an Anisotropic Elastic Body. Holden-Day, Inc., San Francisco.

Mellor, M. (1980). Mechanical properties of polycrystalline ice. In: Tryde, P. (Ed.), Proc. IUTAM Symp. on the Physics and Mechanics of Ice, Springer, pp. 217–245.

Mellor, M. and Cole, D.M. (1982). Deformation and failure of ice under constant stress or constant strain-rate. Cold Regions Science and Technology, 5(2): 201–219.

Mellor, M. and Cole, D.M. (1983). Stress/strain/time relations for ice under uniaxial compression. Cold Regions Science and Technology, 6(2): 207–230.

Miller, A. (1976). An inelastic constitutive model for monotonic, cyclic, and creep deformation: part I – Equations development and analytical procedures. J. Eng. Materials and Technol., 96: 97–104.

Orowan, E. (1946). The creep of metals. J. West Scotland Iron Steel Inst. 54: 45–53.

Palmer, A.C. (1967). Creep-velocity bounds and glacier-flow problems. J. Glaciol., 6(46): 479–488.

Prager, W. (1955). The theory of plasticity: A survey of recent achievements (James Clayton Lecture). Proc. Inst. Mech. Eng. 169(41): 3–19.

Rabotnov, Yu. N. (1969). Creep problems in structural members. English Translation by Leckie, F.A., North Holland Publishing Company.

Shyam Sunder, S., Ganguly, J. and Ting, S.K. (1987). Anisotropic sea ice indentation in the creeping mode. J. Offshore Mech. and Arctic Eng., 109(2): 211–219.

Sinha, N.K. (1978). Rheology of columnar-grained ice. Experimental Mechanics, 18(12): 464–470.

Sinha, N.K. (1979). Grain-boundary sliding in polycrystalline materials. Philosophical Magazine A, 40(6): 825–842.

Sinha, N.K. (1981). Rate sensitivity of compressive strength of columnar-grained ice. Experimental Mechanics, 21(6): 209–218.

Sinha, N.K. (1982). Delayed elastic strain criterion for first cracks in ice. In: Vermeer, P.A. and Luger, H.J. (Eds.), Proc. IUTAM Conf. Deformation and Failure of Granular Materials, A.A. Balkema Rotterdam, pp. 323–330.

Sinha, N.K. (1983). Creep model of ice for monotonically increasing stress. Cold Regions Science and Technology, 8(1): 25–33.

Sinha, N.K. (1987). Effective Poisson's ratio of isotropic ice. Proc. 6th Int. Offshore Mech. Arctic Eng. Symp., Vol. IV, pp. 189–195.

Sinha, N.K., Timco, G.W., and Frederking, R. (1987). Recent advances in ice mechanics in Canada. In: Chung, J.S., Hallam, S.D., Maatanen, M., Sinha, N.K., and Sodhi, D.S. (Eds.), Advances in Ice Mechanics – 1987, ASME, Offshore Mech. Arctic Eng. Symp. Comm., Houston, Texas, pp. 15–35.

Truesdell, C. (1955). Hypoelasticity. Journal of Rational Mechanics and Analysis, 4(1): 83–133.

Wu, M.S. and Shyam Sunder, S. (1988). A rate and pressure sensitive damage model for polycrystalline ice. (In preparation.)